Biochimica et Biophysica Acta 1848 (2015) 266–276

Contents lists available at ScienceDirect

Biochimica et Biophysica Acta

journal homepage: www.elsevier.com/locate/bbamem

Fibrillation of β amyloid peptides in the presence of phospholipid bilayers and the consequent membrane disruption ☆

Wei Qiang [a,b,*], Wai-Ming Yau [b], Jürgen Schulte [a]

[a] Department of Chemistry, Binghamton University, State University of New York, Binghamton, NY 13902-6000, USA
[b] Laboratory of Chemical Physics, National Institute of Diabetes and Digestive and Kidney Diseases, National Institutes of Health, Bethesda, MD 20892-0520, USA

ARTICLE INFO

Article history:
Received 5 February 2014
Received in revised form 24 March 2014
Accepted 13 April 2014
Available online 22 April 2014

Keywords:
Alzheimer's disease
Neurotoxicity mechanism
Membrane disruption
β amyloid fibril
Solid state NMR

ABSTRACT

Fibrillation of β amyloid (Aβ) peptides and the accumulation of amyloid plaques are considered as an important clinical hallmark to identify Alzheimer's disease (AD). The physiological connection between Aβ plaques and the disruption of neuronal cells has not been clearly understood. One hypothesis to explain the Aβ neurotoxicity is that the fibrillation process induces disruption to the cellular membrane. We studied the Aβ fibrillation process in two biologically relevant conditions with the peptide either pre-incorporated into or externally added to the synthetic phospholipid bilayers. These two sample preparation conditions mimic the physiological membrane proximities of Aβ peptides before and after the enzymatic cleavage of amyloid precursor protein (APP). Using thioflavin T (ThT) fluorescence and transmission electron microscopy (TEM), we were able to monitor the kinetics and morphological evolution of fibril formation, which was highly sensitive to the two sample preparation protocols. While the external addition protocol generates long and mature fibrils through normal fibrillation process, the pre-incubation protocol was found to stabilize the immature protofibrils. Fluorescence spectroscopy studies with doubly-labeled phospholipids indicated that there may be a lipid uptake process associated with the fibril formation. Solid state nuclear magnetic resonance (NMR) spectroscopy provided evidence for high resolution structural variations in fibrils formed with different protocols, and in particular the stabilization of long-range contact between N- and C-terminal β strands. In addition, disruption of phospholipid bilayers was supported by measurements with ^{31}P chemical shifts and relaxation time constants. This article is part of a Special Issue entitled: NMR Spectroscopy for Atomistic Views of Biomembranes and Cell Surfaces. Guest Editors: Lynette Cegelski and David P. Weliky.

1. Introduction

One of the most crucial clinical hallmarks for the diagnosis of Alzheimer's disease (AD) is the accumulation of extracellular β amyloid (Aβ) plaques around neuronal cells [1,2]. The elementary building blocks of these plaques are Aβ fibrils, which come from the aggregation of Aβ peptides [3,4]. These peptides are 40- or 42-residue segments generated from enzymatic cleavage of large membrane-associated amyloid precursor protein (APP) [5,6]. Previous liquid state nuclear magnetic resonance (NMR) spectroscopy study on the trans-membrane domain of APP has shown that the Aβ sequence was located at the interior of the membrane bilayer [7]. After cleavage, the peptide should be partially inserted in the membrane and could be eluted from the membrane bilayer. The molecular mechanisms and the trigger of Aβ elution are not fully understood, however, the total amount of cholesterol as well as cholesterol distribution across the membrane bilayer had been considered to have important effects [8]. Aggregation of Aβ which leads to the fibril formation may start after the peptide elution, and the fibrillation process may induce disruption to the membrane bilayer. This has been proposed as one molecular mechanism for Aβ neurotoxicity [8–11].

Previous experiments have demonstrated that Aβ interacts with artificial membrane bilayers, isolated brain membranes as well as plasma membranes in living cells [12–23]. For synthetic membrane with phospholipids, it has been shown that the binding of Aβ can be affected by both the primary peptide sequence and the fluidity and phase of the membrane [12,14,15,24]. Short segments of the peptide with the most hydrophobic part of the primary sequence are more likely to be inserted into the membrane hydrophobic core [12]. The full-length peptides with charged N-terminus could interact with the polar lipid headgroups through electrostatic interactions. Binding of Aβ to synthetic membrane monolayers results in reduced membrane fluidity, probably by forming immobile domains which contained phospholipids and short fibrillar fragments [15]. Conformational change in Aβ upon membrane binding has been monitored using circular dichroism (CD) spectroscopy. It has been shown that the peptide's global secondary structure remains to be random coil if the phospholipid headgroups are neutral. However, regular secondary structures form upon the addition of negatively

☆ This article is part of a Special Issue entitled: NMR Spectroscopy for Atomistic Views of Biomembranes and Cell Surfaces. Guest Editors: Lynette Cegelski and David P. Weliky.

* Corresponding author at: Department of Chemistry, Binghamton University, 4400 Vestal Pkwy East, Binghamton, NY 13902-6000, USA. Tel.: +1 607 777 2298.
E-mail address: wqiang@binghamton.edu (W. Qiang).

http://dx.doi.org/10.1016/j.bbamem.2014.04.011
0005-2736/

charged lipids. A predominant β strand conformation has been observed at intermediate peptide to lipid (P:L) molar ratio (*i.e.* <1:50), while the fraction of α-helical conformation increases with lower P:L [16]. Solid state NMR spectroscopy has been applied as a unique approach to obtain molecular-level information on the membrane interactions of amyloid proteins and antimicrobial peptides [25–27], mainly because the system is naturally non-crystalline and insoluble. The ^{13}C chemical shift measurements on the short segment $A\beta_{29-42}$ have shown a predominant β strand conformation upon binding with P:L that equals to 1:30 [28]. Deuterium NMR has also provided evidence that the methyl group of Ala33 in $A\beta_{29-42}$ G33A mutant interacts with the membrane bilayer. In addition, the ^{31}P transverse relaxation (T_2) time constant analysis has indicated that the peptides were more likely to interact with the negatively charged phosphatidylserine (PS), rather than the neutral phosphatidylcholine (PC) [29].

There is also a large degree of variation in terms of both the peptide locations in membrane bilayers and the change of membrane fluidity when the Aβ is added to isolated brain membranes. The initial binding of the peptide to human plasma membrane surface has been observed using electron microscopy (EM) [17]. Using rat synaptic plasma membrane, it has been shown that the soluble $A\beta_{1-40}$ incorporated into the hydrophobic interior and the non-soluble aggregates had close proximity to the polar headgroup regions, presumably because it was difficult for the aggregates to travel through the membrane. The effect of Aβ on membrane fluidity has not been clearly demonstrated. Some of the previous work have shown that the fluidity of human hippocampal membranes was greatly reduced by the addition of full-length, neurotoxic $A\beta_{1-40}$ or $A\beta_{1-42}$, but was not affected with shorter, non-toxic $A\beta_{1-29}$ [20,21,23]. However, there are also reports on the increase of Aβ disorders and membrane fluidity upon interaction [19,30,31]. For the plasma membrane in living cells, it has been recently shown that the membrane fluidity was significantly reduced by oligomeric Aβ species comparing with fibrillar or monomeric species [22].

Due to the complexity of the Aβ–membrane system, the molecular mechanism of interactions is not well understood, which includes the structural evolution of Aβ from monomeric peptides to fibrillar species and the molecular-level membrane disruption during the fibrillation process. *In vitro* models for studying these molecular mechanisms involve synthetic membrane bilayer with phospholipids. Unlike functional proteins, Aβ fibrils do not have a naturally folded state with global minimum energy. The fibril structures are proved to be very sensitive to external environment, particularly the sample preparation conditions [32–39]. In addition, the elution of Aβ after cleavage may not be the only fate for this peptide. Since it could be inserted into the membrane interior as monomer, it could also be involved in the formation of endosomes [12,19]. For these reasons, we hope to study the Aβ structure in the presence of membrane as well as the membrane disruption using *in vitro* models in a more systematic way. We prepared Aβ/membrane samples using two different protocols. The "*external addition*" protocol added monomeric Aβ peptides into preformed phospholipid membranes, which mimic the scenario where there was an extracellular aggregation process. The "*pre-incorporation*" procedure, on the other hand, generated phospholipid vesicles with Aβ embedded beforehand. This procedure may simulate the case where there is membrane-bound Aβ. The latter case could also happen when there is a formation of cholesterol-enriched lipid domains, which tends to increase the local concentration of Aβ [18,40]. Effects of sample preparation on peptide conformation and membrane interactions have been noticed previously. It has been shown by CD spectroscopy that the "*pre-incorporation*" procedure stabilizes the global α-helix conformation of Aβ within a time period of several weeks, while for the "*external addition*" samples, the peptides experienced a conformational conversion from random coil to β sheet within two weeks [41]. In addition, static solid state NMR ^{31}P spectroscopy has suggested that the "*pre-incorporation*" procedure induced an increased intensity of isotropic peak, which means disruption of the bilayer structures and formation of small spherical lipid construct like micelles. The external addition of Aβ does not change the membrane global structure [29].

To start answering the question of the molecular mechanisms of membrane disruption induced by Aβ fibrillation, it is crucial to monitor the membrane disruption effect in the same time course as the fibrillation process. Previous work on the islet amyloid polypeptide (IAPP) utilizes synchronized fluorescence measurements for both fibrillation and leakage of membrane contents [42]. In addition, it has been shown that the detailed phospholipid compositions might have significant effects on the aggregation of amyloid proteins, presumably due to the change in membrane curvature [43]. In this present work, we utilized thioflavin T (ThT) fluorescence spectroscopy to monitor the fibril formation kinetics, and double-fluorophore-labeled phospholipids to study the membrane disruption effect. The later approach has been widely used to study the membrane fusion kinetics. Meanwhile, transmission electron microscopy (TEM) was applied in a time-synchronized fashion to follow the morphological evolution of the Aβ fibrillation process. Solid state NMR spectroscopy was used to study the molecular-level structural difference of Aβ fibrils from different sample preparation conditions, as well as the change in membrane structures.

2. Materials and methods

2.1. Peptide synthesis

Unlabeled $A\beta_{1-40}$ for fluorescence and TEM studies, and $A\beta_{1-40}$ with ^{13}C, ^{15}N-uniform labeling at residues Phe19 and Leu34 for NMR studies, were both synthesized on solid phase peptide synthesizer (Applied Biosystems Inc., Foster City, CA) with standard Fmoc chemistry. The peptide was then cleaved from supported resin using trifluoroacetic acid (TFA) cleavage mixture (TFA/phenol/water/thioanisole/EDT, 82.5/5/5/5/2.5) and purified using high performance liquid chromatography (HPLC, Beckman-Coulter Inc., Brea, CA) with reversed-phase C18 column. The purity of both peptides was proved to be >95% using matrix-assisted laser desorption ionization (MALDI) time-of-flight (TOF) mass spectrometer (Shimadzu Scientific Instrument Inc., Columbia, MD).

2.2. Liposome preparation

In both "*pre-incorporation*" and "*external addition*" protocols, the molar ratio of P:L equals 1:20. Four different types of lipid mixtures were utilized for each sample preparation method with different fractions of negatively charged headgroups and/or the content of cholesterol. The lipid mixtures were: 100% 1-palmitoyl-2-oleoyl-*sn*-glycero-3-phosphocholine (POPC, from Avanti Polar Lipids Inc., Alabaster, AL); 80% POPC plus 20% 1-palmitoyl-2-oleoyl-*sn*-glycero-3-phospho-(1′-*rac*-glycerol) (POPG); 80% POPC, 20% POPG plus additional 30 mol% cholesterol (CH); and total brain extract. These samples were named as PC, PC/PG, PC/PG/CH and BR hereafter. The negatively charged phospholipids have been reported to increase the Aβ absorption to the liposome [29]. Cholesterol has been proposed as an important component involving Aβ binding as well as membrane elution [7,18,40]. In addition, the brain extract was utilized to mimic the membrane composition *in vivo*. For "*pre-incorporation*" samples, the designed amounts of lyophilized $A\beta_{1-40}$ peptide and phospholipid mixtures were co-dissolved in hexafluoro-2-propanol (HFIP). The solution was sonicated in a water bath for 5 min to ensure the complete dissolving and then the solvent was removed with N_2 flow. The remaining lipid/peptide film was dried in a desiccator overnight and rehydrated using 10 mM phosphate buffer (pH 7.4, containing 0.01% NaN_3). Peptide concentration was kept at 25 μM to avoid the formation of large aggregation during the time period of vesicle preparation. Re-suspended lipid/peptide mixture was agitated vigorously for 1 h at ambient temperature. The solution containing mainly multilamellar vesicles (MLVs) was then incubated at 37 °C for fibrillation. For "*external addition*" samples, all MLVs were pre-formed using the same protocols as provided above without

peptides. The Aβ peptides were then dissolved in dimethyl sulfoxide (DMSO) and diluted into vesicle solutions so that the final concentration of peptide was 25 μM. There was ~1% (v/v) DMSO in the final MLV solution.

2.3. Fluorescence spectroscopy

For the fibrillation kinetics measurements using ThT, a 10 μL aliquot of Aβ/vesicle solution was added into 100 μL of 10 mM ThT solution, and the fluorescence emission was recorded at 490 nm with excitation wavelength of 423 nm. The sample aliquots were taken from Aβ fibrillation solution at different time points for both "*pre-incorporation*" and "*external addition*" samples. Control experiments were done with MLVs formed using the same lipid mixtures without peptides.

For the measurements to identify membrane disruption, 2 mol% of fluorophore-labeled lipids, 1,2-dipalmitoyl-*sn*-glycero-3-phosphoethanolamine-N-(7-nitro-2-1,3-benzoxadiazol-4-yl) (NBD-PE) and 1,2-dipalmitoyl-*sn*-glycero-3-phosphoethanolamine-N-(lissamine rhodamine B sulfonyl) (Rh-PE), were incorporated into the total lipid mixtures. These double-fluorophore-labeled vesicles have been previously utilized to study the membrane fusion process induced by the human immunodeficiency virus (HIV) fusion peptides [44,45]. Excitation of the NBD fluorophore at ~470 nm results in an emission at ~535 nm, which overlaps with the excitation wavelength of Rh fluorophore. The induced fluorescence emission at ~585 nm was detected and the change of emission intensity was related to the proximity between two fluorophore groups. Each assay contained 90% of unlabeled vesicles and 10% of double-fluorophore-labeled vesicles. An aliquot of 100 μL Aβ/membrane solution was taken out for measurement at the time points determined by fibrillation. Control experiments without peptides were done to calibrate the effect of spontaneous lipid mixing. Both types of fluorescence measurements were conducted on fluorimeter (StellarNet Inc., Tampa, FL) with single wavelength diode light sources. The emission signal was collected with 1000 ms signal averaging.

2.4. Transmission electron microscopy

All negatively-stained TEM measurements were completed on a FEI Morgagni Electron Microscope. An aliquot of 10 μL Aβ/membrane solution was deposited on a TEM sample grid (Ted Pella Inc., Redding, CA) coated with a thin layer of carbon film for 2 min. The solution was blotted and then the grid was washed once with 10 μL deionized water. After removing the water, the grid was stained with 10 μL of 3% uranyl acetate for 35 s and subject to measurements.

2.5. Solid state NMR

Fibrils were allowed to grow for at least 2 weeks before the samples were collected. TEM images were recorded to verify that there was no further morphological evolution of fibrils at the time point of sample collection. For NMR sample preparation, Aβ/membrane solution was pelleted down with ultracentrifugation at 432,000 ×*g* (Beckman Coulter Inc., Brea, CA) for 1 h at 4 °C. The wet pellet was frozen and transferred into magic angle spinning (MAS) solid state NMR rotor without lyophilization to avoid any disruption of membrane structure due to the dehydration process.

Two-dimensional (2D) $^{13}C/^{13}C$ spin diffusion experiments were performed on a 9.4 T Varian (Agilent Technologies Inc., Santa Clara, CA) solid state NMR spectrometer with a 3.2 mm HXY triple resonance magic angle spinning (MAS) probe. Spectra were collected with 1.5 s recycle delay, 500 ms radiation assisted diffusion (RAD) period, 10.0 kHz MAS frequency, 50 kHz ^{13}C cross polarization (CP) field with linear ramp and ~100 kHz ^{1}H decoupling field. All NMR experiments were done with −10 °C cooling air to prevent dehydration, and the actual sample temperature was ~20 °C. The sample temperature and dehydration levels were verified by detecting the ^{1}H chemical shifts and signal intensities before and after experiments. All 2D spectra were processed with 150 Hz Gaussian line broadening in both dimensions.

The static and MAS ^{31}P spectra were collected on a 14.1 T Bruker (Bruker Biospin Corp., Billerica, MA) NMR spectrometer equipped with a 2.5 mm TriGamma MAS probe. Similar to the ^{13}C experiments, samples were protected from dehydration throughout the experiment using cooling air. The static ^{31}P experiments were done without sample spinning and the ^{31}P T_2 relaxation measurements were completed with Hahn Echo pulse sequence (90°-τ–180°-echo) with 50 kHz radiofrequency (*rf*) pulses and 100 kHz ^{1}H decoupling. Each ^{31}P spectrum was acquired with 64 scans and processed with 20 Hz Gaussian line broadening. Samples were spinning at 10.0 kHz for all measurements. All spectra were referenced to the ^{31}P chemical shift of 80% H_3PO_4 at 0.0 ppm. Experimental data were fit to a single exponential decay curve.

3. Results

3.1. Morphological evolution of Aβ fibrils in different sample preparations

Fig. 1 showed the evolution of Aβ morphology along with the fibrillation process. Typically in similar process without the membrane, the peptide will experience certain lag period when nucleation happens [46,47]. Small Aβ aggregates may form during the lag period, however their presence may not be detected using TEM. As had been previously demonstrated, at the experimental Aβ concentration, *i.e.* 25 μM, the fibrillation process will not be detectable using TEM within at least 4 h in the absence of membranes [48]. Fig. 1A–E showed the time-evolution of sample morphology for the "*pre-incorporation*" samples, and it was clear that curvy and short fibrillar species were observed even at the very beginning stage of fibrillation process, *i.e.* 4 h. Although the fibril length increases over time, the curvy morphology, which is typically for protofibrils, did not have significant change for samples incubated up to 2 weeks. Meanwhile, the morphology of vesicles seemed to be affected from the beginning of fibrillation, where disintegration of membranes was observed. For "*external addition*" samples, on the other hand, formation of fibrils was not detected until incubation for 46 h. Mature fibrils with long-filament-like morphology were observed from 69 to 93 h. It also seems that the detailed fibrillation kinetics was affected by the phospholipid components of LMVs. For LMVs with total PC/PG/CH and BR, a clear morphological evolution pathway was observed. During the process, small oligomers in spherical shape were first observed around membrane surface. These spherical species were converted into curvy protofibrils which gradually made connection between vesicles (Fig. 1H), and finally the curvy morphology changed into straight and long. For LMVs with PC and PC/PG, such pathway was not observed, and linear filaments were directly observed after approximately 70-hour incubation (Fig. S1). This difference suggested that fibril formation kinetics was affected by the membrane composition, presumably related to the change in local concentration of Aβ. This was consistent with previous observation in human cortex membranes that Aβ aggregates were concentrated in membrane regions with large cholesterol content [18]. However, this does not necessarily mean that the presence of cholesterol accelerated the nucleation. In fact in all cases, nucleation, which was defined by the increase in ThT fluorescence intensities, started immediately after the addition of peptides into vesicle solutions.

The final morphologies of both LMVs and Aβ fibrils were different for the two sample preparation approaches, but were similar for different lipid mixtures within one sample preparation protocol. The "*external addition*" fibrils were long and straight, typically in length of several microns. The "*pre-incorporation*" fibrils only extended to several hundreds of nanometers within two weeks and the morphology remains curvy. The morphological feature of "*pre-incorporation*" fibrils was very similar to a previously observed metastable intermediate formed by the Iowa mutant of Aβ. It was possible that the curvy filaments in the present

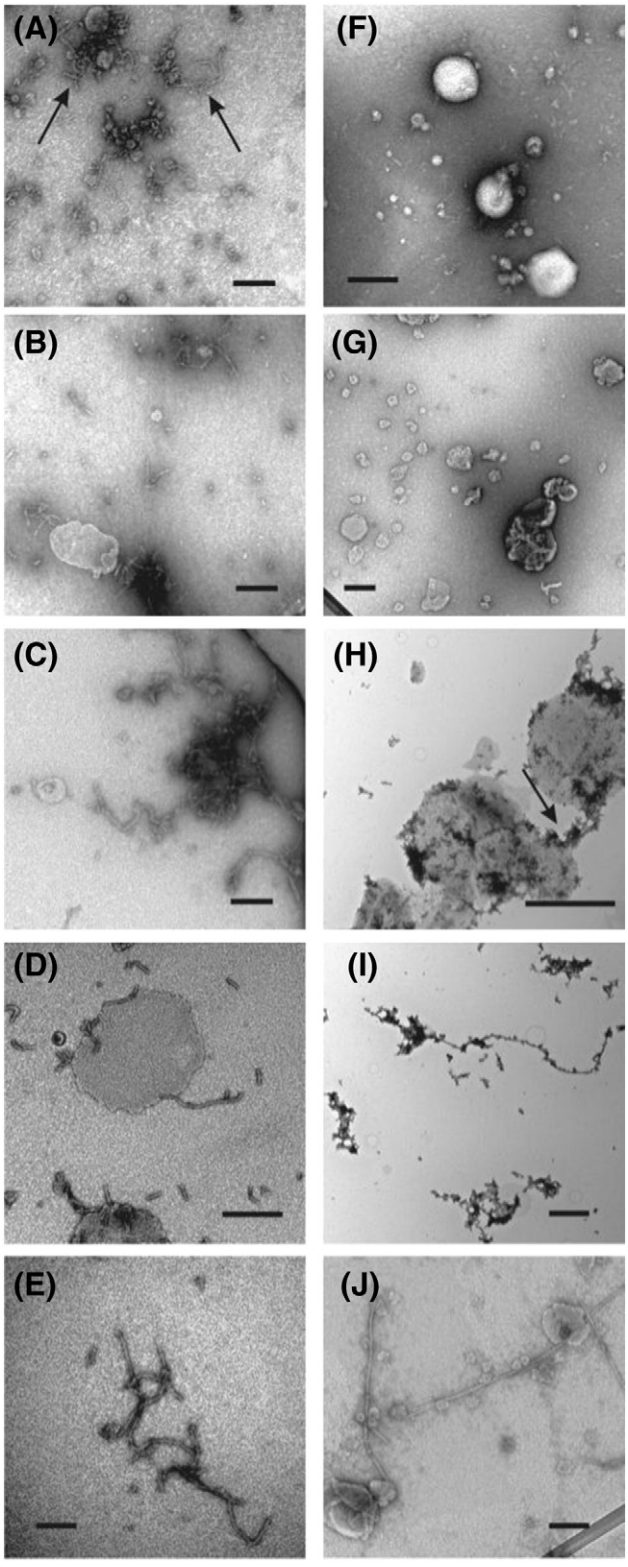

Fig. 1. Morphological evolution of Aβ/membrane systems prepared with (A–E) "*pre-incorporation*" and (F–J) "external addition" sample preparation protocols using vesicles with lipid mixture PC/PG/CH. TEM images were taken at (A and F) 4 h, (B and G) 22 h, (C and H) 46 h, (D and I) 69 h and (E and J) 93 h after the initiation of fibrillation. Arrows in panel A indicated the formation of curvy filaments at the early stage of "pre-incorporation" protocol, and arrows in panel H showed the fibril that connects two vesicles. The scale bars were 100 nm in all images.

work also represented an intermediate structure. Previous study has shown that the presence of membrane would induce fragmentation of mature lipids and the stabilization of short segments [15], which might explain the maintaining of curvy morphology in "*pre-incorporation*" samples. In addition, there was also difference in terms of the membrane morphology. Predominant spherical vesicles were observed throughout the fibrillation process in "external addition" samples, while disintegrated membrane fractions were detected at the very beginning stage of "*pre-incorporation*" sample preparation (Fig. 1A).

3.2. Fibrillation kinetics was distinct for different protocols

ThT fluorescence was recorded at different time points during the fibrillation process, and the plots shown in Fig. 2 were calibrated by subtracting the fluorescence of vesicle solutions without peptides at the same time points. For the control sample, we observed very little change of fluorescence intensity as a function of incubation time, however the absolute values of emission intensity were dependent on the lipid mixture components (Fig. S2). The presence of PG greatly enhanced the fluorescence emission, while the presence of cholesterol seemed to induce the decrease of the fluorescence intensity.

The overall fibril growth kinetics varied dramatically for the two sample preparation protocols. The "*external addition*" samples showed slow increase within the first 5 days of incubation, and a more rapid fluorescence enhancement after one week. The fluorescence emission signal leveled off for all four types of lipid mixtures after two weeks of incubation. The "*pre-incorporation*" samples, on the other hand, had rapid signal increasing at the beginning stage of fibrillation (*i.e.* from 4 to 43 h) but quickly leveled off thereafter. There was little further change in fluorescence intensities up to two weeks. These results clearly suggested different fibrillation pathways for the two sample preparation protocols. Lag period without detectable fluorescence signal was not observed in either case, which was different for wild-type Aβ fibrillation process without the membrane [49]. For the "*external addition*" protocols, the initial slow increase of ThT fluorescence may indicate a complicated process including the absorption of Aβ to the membrane surface, concentration of the peptide to form aggregates, and the conformational evolution that led to further fibril elongation. For the "*pre-incorporation*" samples, small oligomeric states of Aβ might already exist at the beginning of incubation, which means that the structural transition for fibril elongation may only happen within the preformed oligomers, *i.e.* only re-arrangement of Aβ monomers was involved. In this case, there might be no requirement for recruiting monomers from extra-membrane solution to reach a critical concentration. However, after the formation of the appropriate peptide conformation, further elongation required sufficient contact between the short fibril segments (*i.e.* seeds) and monomeric peptides. For "*external addition*" samples, this was more straightforward because the seeds were probably located on the membrane surface. However, the "*pre-incorporation*" fibril seeds may be buried in membrane bilayers or interact with phospholipids, which made further elongation process more difficult. Certain metastable structures may be stabilized simply because the energy cost for breaking the existing interactions (presumably between fibrils and membranes) was larger.

The absolute values of fluorescence emission intensities at equilibrium were determined by subtle changes in high resolution structures of Aβ fibrils [35,50], and were difficult to interpret without knowledge of structures. However in general, it was clearly shown that fibril structures were sensitive to phospholipid components, which suggested that for the mechanism studies using *in vitro* models, it was important to consider the lipid content change and to use biologically relevant lipid mixtures.

3.3. Membrane disruption occurred simultaneously with fibrillation

To understand the membrane disruption kinetics and mechanisms, we introduced two types of fluorophore-labeled phospholipids,

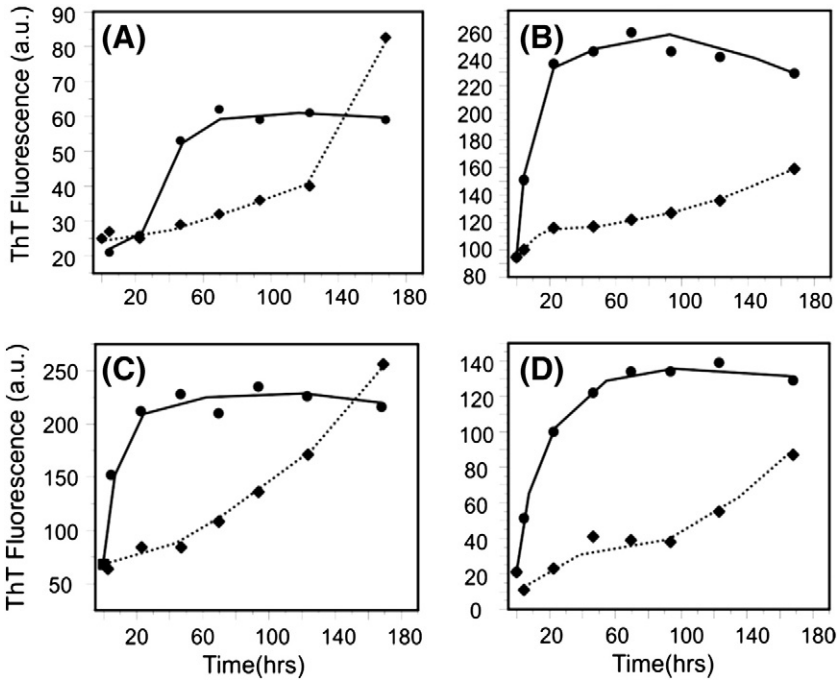

Fig. 2. Detection of thioflavin T (ThT) fluorescence emissions as the function fibrillation time for Aβ/membrane systems with the phospholipid compositions of (A) PC, (B) PC/PG, (C) PC/PG/CH and (D) BR. In each plot, circles and diamonds indicated the "*pre-incorporation*" and "*external addition*" sample preparation conditions, respectively.

NBD-PE and Rh-PE. Excitation of NBD group results in fluorescence emission of Rh group through the Forster resonance energy transfer (FRET) mechanism. The assay was designed to detect membrane fusion process. Since the labeled LMVs were diluted into unlabeled vesicles, as the fusion happens, the distance between two fluorophores became longer and the fluorescence intensity at the emission wavelength of Rh-PE (*i.e.* ~585 nm) would decrease. Fig. 3 showed the time course of emission intensities for different samples at 585 nm. The plots were corrected by subtracting the fluorescence changes only due to the vesicles using control samples, which were very little (Fig. S3). Surprisingly, a general trend of signal increasing rather than decreasing was detected for all samples. To exclude the possibility of membrane fusion, we did another control experiment by adding 1% Triton directly into the vesicle solution. The results (Fig. S4), with an increasing intensity at 530 nm and decreasing intensity at 585 nm, clearly indicated the occurrence of membrane fusion. Therefore, we concluded that the $A\beta_{1-40}$ was not fusogenic, which was different from the shorter segment $A\beta_{29-42}$ that has been proposed previously [51].

Similar to the fibrillation kinetics profiles, the membrane disruption kinetics was also distinct for the "*external addition*" and "*pre-incorporation*" samples. More importantly, the time courses for the two sets of fluorescence measurements showed a synchronized fashion, *i.e.* the build-up curves for "*pre-incorporation*" samples were much rapid comparing with the "*external addition*" samples. All "*pre-incorporation*" curves leveled off at ~22 h, which corresponded to the rapid increase of ThT fluorescence signals during the same time period. On the contrary, increase of Rh-PE emission matched with the initial ThT signal, but leveled off after ~100 h. In addition in both protocols, membrane disruption started immediately with the fibrillation process. The results suggested that the process of Aβ initial aggregation leading to fibrillar seeds was probably crucial for membrane disruption. For the "*external addition*" case, the Rh fluorescence intensities leveled off during the time period of rapid ThT fluorescence enhancement (*i.e.* the time period after ~100 h), meaning that the elongation of mature fibrils might have little effect on the membranes. It has been recognized that it was the Aβ oligomers rather than mature fibrils that have shown highest neurotoxicity [52,53]. The combination of ThT and Rh fluorescence seemed to suggest that there were certain structural conversions at the beginning stage of fibrillation which are responsible for the membrane disruption.

The observation of Rh fluorescence increasing also provided hints about the detailed mechanisms of membrane disruption. It has been proposed that the fibrillation process can uptake phospholipids from membrane bilayers [54]. Leakage of phospholipids along with the initial fibrillation process provided a possible explanation for the observation that the distance between Rh and NBD groups within one vesicle was getting closer. Another possible explanation involves the formation of cation-selective channels formed by membrane fragmentation, which corresponds to the two-step membrane disruption mechanism proposed previously [55,56]. The fragmentation may also reduce the size of liposomes, and therefore decrease the proximities between fluorophore-labeled lipids. These possibilities will be investigated in future studies.

3.4. High resolution structural variation in different fibrils and membrane disruption

Solid state NMR 2D $^{13}C/^{13}C$ spin diffusion experiments were performed to understand the detailed structural difference between different sample conditions. The $A\beta_{1-40}$ fibrils were labeled with U-^{13}C, ^{15}N-Phe19 and Leu34. These two residues were chosen because they were located in the hydrophobic core region of all previously published fibril structures and there was potential strong contact with resolved NMR cross peaks between them [32,57–59]. Meanwhile, the chemical shifts of Phe19 are sensitive to sample preparation conditions.

Fig. 4 showed the representative 2D NMR spectra with the lipid mixtures PC/PG/CH and BR in vesicles. Two major differences were observed. First of all, within the same membrane, the "*external addition*" samples gave stronger long-range contact (*i.e.* the Phe19/Leu34 crosspeak) comparing with the "*pre-incorporation*" samples. The result indicated that the "*pre-incorporation*" protocol generated fibrils with less well-ordered structures, and probably the contact between N- and C-terminal β strands was not well stabilized. Since the two labeled residues were located in the hydrophobic core in mature fibrils, it was possible that the "*pre-incorporation*" fibrils contained structures that have

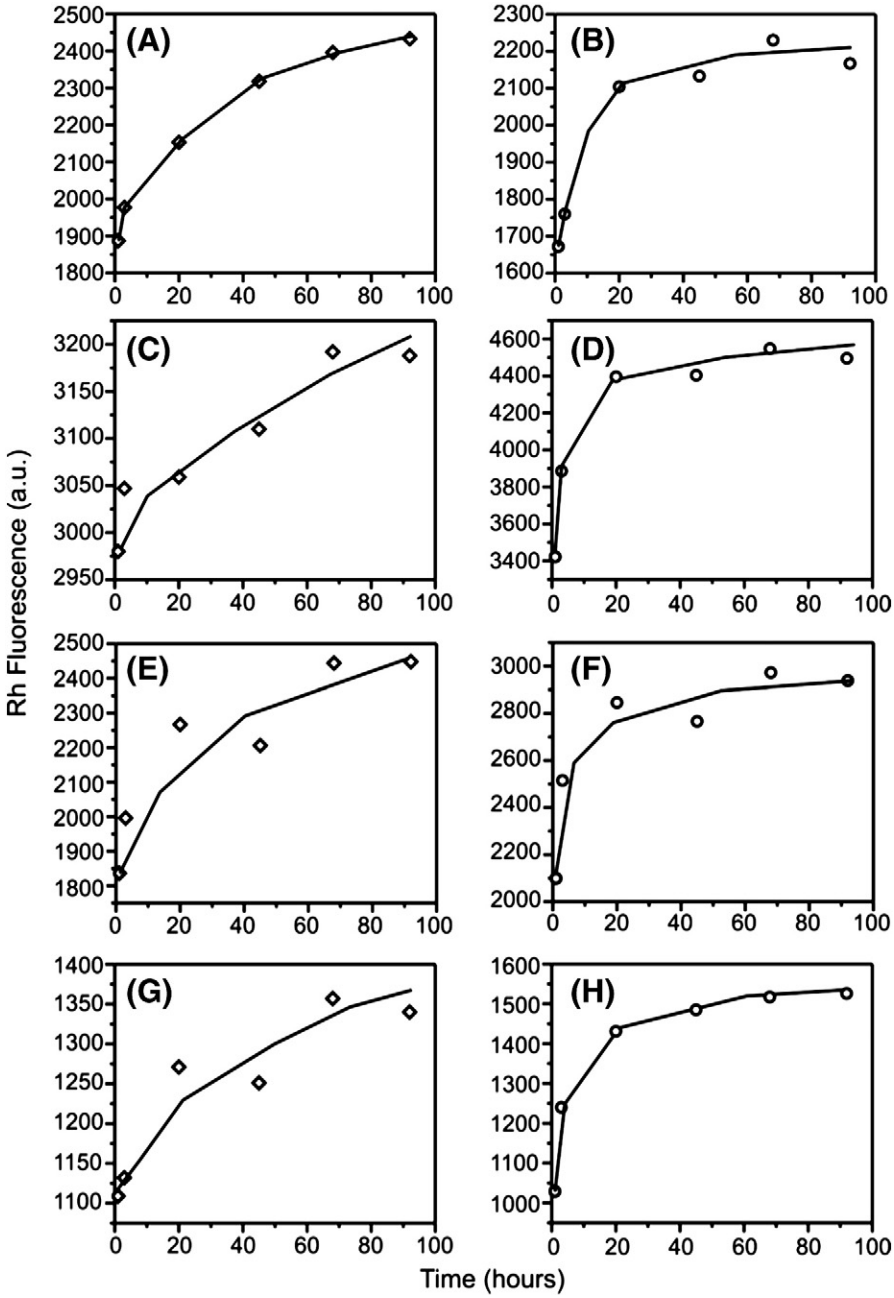

Fig. 3. Detection of Rh-PE fluorescence emissions as the function of fibrillation time using Aβ mixing with 2 mol% doubly-fluorophore-labeled vesicles. Different lipid mixture components were shown as (A and B) PC, (C and D) PC/PG, (E and F) PC/PG/CH and (G and H) BR. The panels A, C, E and G were for "*external addition*" samples and the panels B, D, F and H were for "*pre-incorporation*" samples.

not been well folded. This was consistent with the difference in TEM images, where the "*external addition*" fibrils were more mature. Second, the Cα and Cβ chemical shifts of Phe19 changed between samples prepared using the same protocol but with different membrane components, but the chemical shifts for Leu34 were the same (Fig. 4A and B). The difference in detailed structure may explain the variation in ThT fluorescence between samples, particularly because the ladder formed by Phe19 aromatic ring along the fibril axis was proposed as a binding site for ThT molecule [60,61]. The ^{13}C linewidths for the two sample preparation protocols were very similar (Fig. 4E and F), despite of the large difference in sample morphologies. For fibril formed with the membrane, it was observed that the ^{13}C linewidths were narrower for mature fibrils comparing with protofibrils [35,59]. There might be extra broadening of linewidths due to the interaction between fibrils and membranes.

^{31}P static and MAS spectra provided additional information about the membrane disruption due to different sample preparation protocols. Our results showed that the ^{31}P chemical shift anisotropy (CSA) for the "*external addition*" samples was ~30% broader comparing with the corresponding "*pre-incorporation*" samples (Fig. 5A–B). This was consistent with a similar previous study using 42-residue Aβ fibrils [29]. In addition, the "pre-incorporation" protocol increased the fraction of isotropic ^{31}P peak in the powder pattern, which was an indication for the formation of smaller vesicles with rapid tumbling. The MAS spectra for the "external addition" PC sample resulted in a single peak at ~−1.9 ppm, while the "pre-incorporation" PC sample contained an additional minor peak at ~−0.8 ppm (Fig. 5C–D). This means that a small fraction of phosphatidylcholine molecules were located in a different chemical environment other than the initial phospholipid vesicles. This second chemical environment might be due to the formation

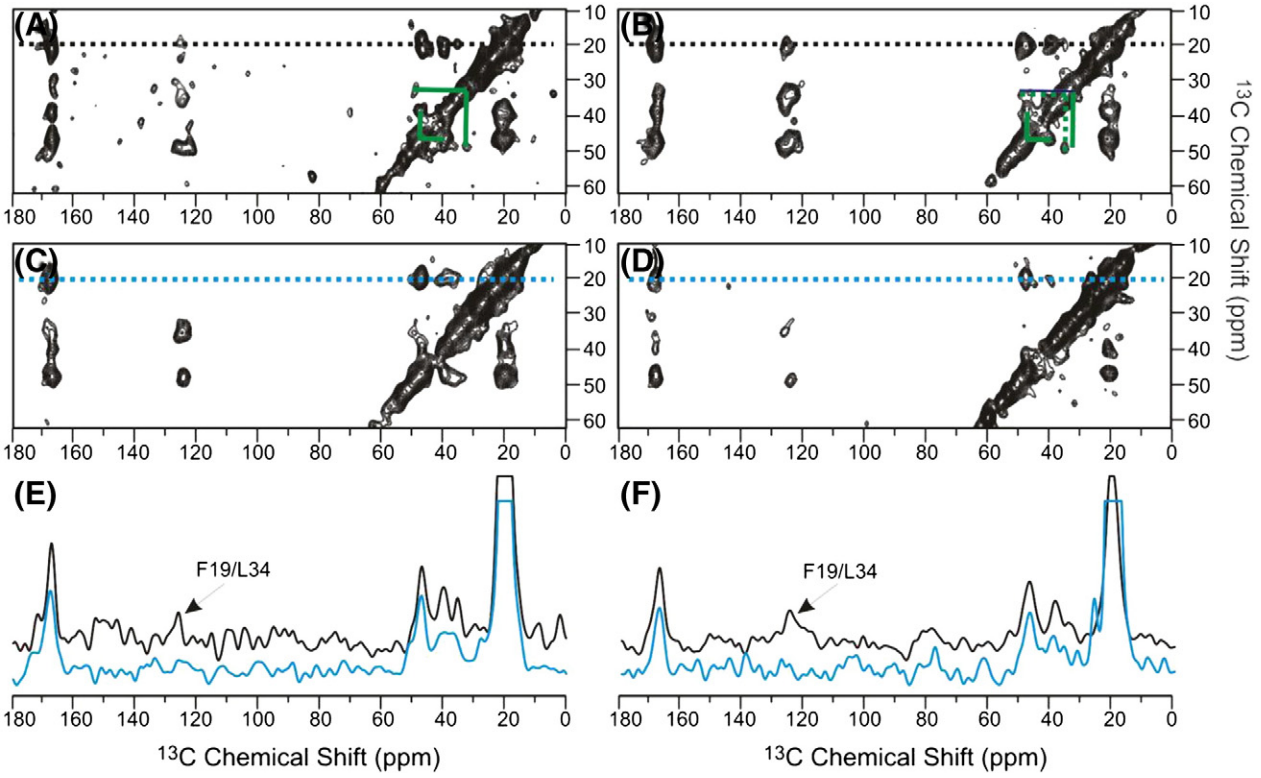

Fig. 4. Two-dimensional (2D) $^{13}C/^{13}C$ spin diffusion solid state NMR spectra for samples prepared with (A and B) "*external addition*" protocols and (C and D) "*pre-incorporation*" protocols. The represented spectra were shown for vesicles with (A and C) PC/PG/CH and (B and D) BR. Horizontal dotted lines were drawn across the chemical shift of Leu34 Cγ1 to highlight the inter-residue crosspeaks between Leu34 and Phe19 in "*external addition*" samples. Corresponding one-dimensional slices were shown in panels E and F for PC/PG/CH and BR, respectively. The green solid lines in panel A indicated the chemical shifts for Cα/Cβ crosspeaks for the two residues. The green dotted lines in panel B showed that there was a shift in Phe19 Cα/Cβ crosspeak position, but not in Leu34.

of smaller phospholipid vesicles because of the membrane fragmentation process, or the formation of peptide–lipid aggregates [29]. The fact that this minor component only existed in "pre-incorporated" sample may indicate that such sample preparation protocol had more significant disruption effects to membranes comparing with the "external addition" protocols, presumably due to the higher local Aβ concentration in membrane. The T2 relaxation time constants for these two peaks were also distinct. While the relaxation constant for the main peak remained at ~1.0 ms, the minor peak showed a much slower decay constant at ~2.7 ms. The presence of two ^{31}P populations with distinct T_2 time constants were observed for PC peak in other vesicle components such as PC/PG and PC/PG/CH (shown in Fig. S5). The analysis for BR samples was not performed because of complexity of lipid headgroup compositions. Since long T_2 indicates higher mobility of ^{31}P lipid headgroup, this result again illustrated that a small population of PC were involved in a construct with high mobility.

4. Discussion

4.1. In vitro models for studying neurotoxicity mechanisms

The aggregation process of Aβ peptides is directly related to the molecular mechanisms of neurotoxicity, and particularly the membrane disruption process. However, since the fibrils are misfolded aggregates, it is unlikely that there is a well-defined folded state like other functional proteins. This means that the detailed structures can be very sensitive to external environments during the fibrillation process, which gives extra difficulties for molecular mechanism studies using *in vitro* models. Based on our results, we emphasize that it is crucial to find model systems that represent the biologically relevant conditions, because subtle changes in high resolution structures of fibrils can lead to dramatic difference in macroscopic characteristic such as ThT binding. A large part of diagnosis strategy for Alzheimer's disease relies on the fluorescent signal intensities from certain agents binding to the Aβ fibrils or plaques. The results could be misleading if the detailed binding mechanisms is not understood, especially when the amyloid plaques contain fibrils with multiple high resolution structures.

Our results also show that it is important to study the molecular details of membrane disruption mechanisms as a function of time. Current arguments about the relative neurotoxicity levels for different fibrillar species (*i.e.* monomers, oligomers, protofibrils and mature fibrils) focus on the measurements of neurotoxicity levels at static states, and the discrepancies were obvious. For instance, it was thought that the mature fibrils had lower toxicity comparing with oligomers/protofibrils if both of them were added directly into the cell culture [62–64]. However, when mature fibrils were sonicated and broke into short pieces, they had comparable toxicity level as protofibrils [59,65]. Since sonicated fibril seeds may still undergo structural evolution, we suspect that the time evolution of structures, rather than the static states, could be more important. In this work, we utilized three different approaches including TEM, ThT fluorescence and Rh fluorescence to track the fibrillation and membrane disruption process, and observed the potential correlation between them. Particularly, the time courses of two types of fluorescence build-up curves that match with each other suggested that the initial structural evolution of Aβ may induce the major membrane disruption. For the "*external addition*" samples, this initial aggregation process may include the absorption and concentration of Aβ on the membrane surface, as well as the consequent structural change to form fibril seeds. There have been reports on the conformational change of Aβ from random coil to partially α-helix, and finally became predominantly β-sheet upon membrane binding [41]. Such structural evolution may change the molecular-level interaction between peptides and membranes, *i.e.* different residues may be exposed to membrane surface at different peptide conformations. For the "*pre-incubation*" samples,

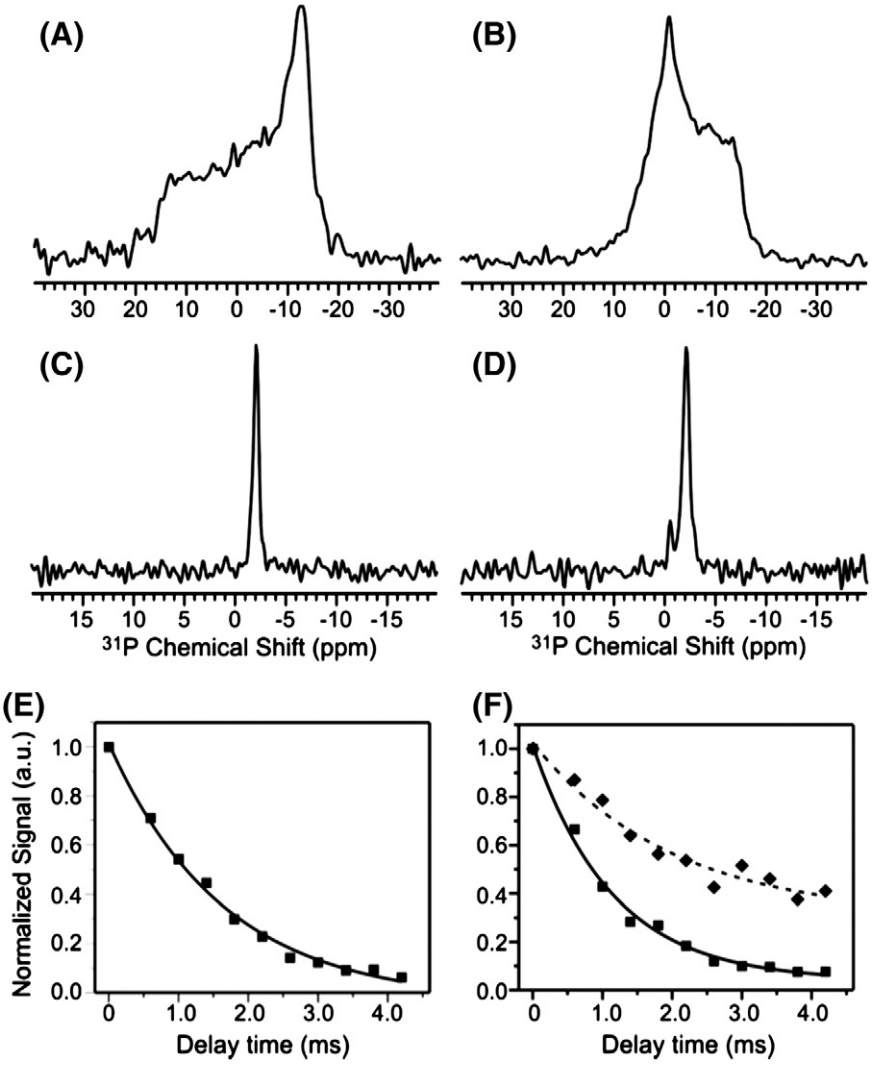

Fig. 5. The ^{31}P static, MAS solid state NMR spectra and T2 relaxation measurements for the (A, C and E) "*external addition*" and (B, D and F) "*pre-incorporation*" samples with PC vesicles. Squares and diamonds in panel F represented relaxation curved for the major and minor peaks in panel D, respectively. Experimental data were fit to single exponential decay curves.

certain oligomeric Aβ states may form at the beginning of fibrillation. Specific interaction between lipids and oligomers might exist to stabilize such oligomers, and these interactions could be disrupted during the fibrillation process, which may further induce destabilization of membrane integrity.

To deeply understand the molecular mechanisms, high resolution techniques such as solid state NMR spectroscopy have to be involved. Solid state NMR has been proved to be extremely successful in solving the atomic-level structures of mature fibrils [36]. On the other hand, it is also a "low sensitivity" technique that is not suitable for tracking the intermediate structures during the fibrillation process. One possibility is to freeze-capture these intermediates at appropriate time points [66], which can be monitored using other complementary approaches such as TEM. However, the potential problem is that the interested intermediate may only be a small fraction within a complicated mixture with multiple structures, and it is difficult to identify the minor peaks from a mixture of NMR signals. Our results with ThT fluorescence indicated that at least for the "*external addition*" samples, there was a slow process from the initial Aβ aggregation to the elongation of mature fibril. This process was characterized by the slow increase of ThT fluorescence emission. This was also the time period that showed the most rapid Rh fluorescence enhancement, which was an indication of membrane disruption. Since the ThT fluorescence is sensitive to very subtle structural variation, we propose that there may be a structural evolution during the time period and it leads to the major membrane disruption. After the initial conformational change, the elongation of mature fibril will take place and this seemed to have less effect on membranes.

Fig. 6 showed an alternate approach to study the intermediate Aβ structure and possible neurotoxic structural evolution. Using known solid state NMR structures for the mature fibril, it is possible to design molecules that can bind and block the elongation pathway. For the simplest scenario, if we assume that there is a competition between two species. One of them has faster nucleation rate, but the nucleus (*i.e.* fibril seeds) is not as stable as the other species. The blocking molecule is designed based on the later species' structure because this will be the one to form mature fibril. When the blocking agents were added to the initial fibrillation system, it will selectively bind to any structural domain that transforms to the more stable species. In other words, it will stabilize the intermediate which will otherwise get converted. This is similar to the usage of conformational-specific antibodies for the structural studies of Aβ oligomers [67]. However, since the blocking agents were designed from specific structural model, this approach could be more selective and more suitable for study detailed structural evolution rather than bulk change in morphology. It is also a potential approach to study the structural evolution during the fibrillation process because of the use of the blocking agent, we should be able to capture the intermediate that is actually on-pathway.

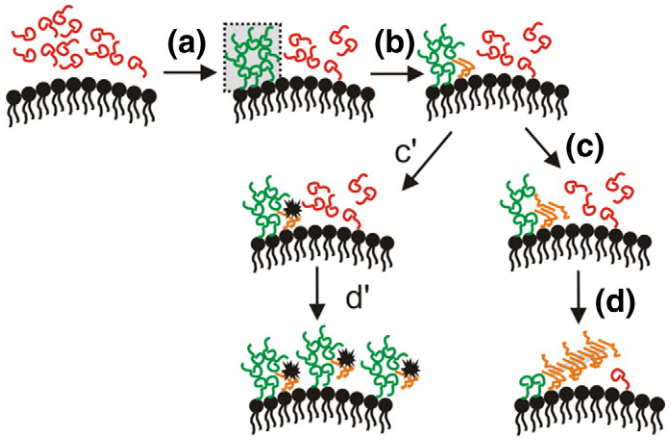

Fig. 6. Models for the Aβ fibrillation in the presence of phospholipid membrane bilayers in the "*external addition*" protocols. The key steps may include (a) absorption and concentration of Aβ on membrane surface, (b) conformational conversion to the structure that is more suitable for elongation, (c) formation of fibril seeds and (d) chain elongation to form mature fibrils. An alternative pathway shows that if a structural-specific blocking agent is added at the beginning stage of fibrillation, there will be (c′) blocking of structural domains with elongation potentials and (d′) equilibrium shifting to the intermediate structures.

4.2. Mechanisms of membrane disruption

It remains a question how exactly membrane bilayers get disrupted by Ab oligomers and fibrils. There have been a number of different mechanisms involved in the interactions between fibrils and membranes. First of all, the fibrillation process may uptake phospholipids. It has been previously reported that for the islet amyloid polypeptide (IAPP) which is associated with type II diabetes, the fibrillation process was accompanied by the association of lipids onto the fibrils [54]. Our results here suggested that the association was more likely to happen during the initial structural evolution stage rather than the elongation stage. Particularly for the "*pre-incorporation*" fibril, the association between lipids and peptides may tend to stabilize the non-fibrillar or protofibril structures, and prevent the formation of mature filaments. It has also proposed that there are formation of specific ionic channels (*i.e.* Ca^{2+} ion channels) with Aβ oligomers. This hypothesis was supported by atomic force microscopy (AFM) observation on channel-like morphology as well as the electrophysiological studies on the voltage jump across synthetic membranes due to the Aβ incorporation [68]. Our results with "*pre-incorporation*" models did not exclude the possibility for the formation of trans-membrane Aβ oligomers or Aβ ionic channels. In fact, previous work with the Aβ Ca^{2+} ion channel did utilize the sample preparation approach similar to our protocol, but with lower P:L ratio. It was likely that the "*pre-incorporation*" system contained a mixture of protofibrils and membrane-bound oligomers.

4.3. Aβ aggregation pathway in the presence of the membrane

In biological systems, Aβ was cleaved from larger APP in the middle of the membrane bilayer, and the hydrophobic C-terminus of the Aβ sequence was partially inserted into the bilayer interior right after the cleavage. The peptide segment could be eluted from the membrane and enter the extracellular fluid immediately because the charged C-terminus would not be preferred in the hydrophobic center. Aβ aggregates may be cleaned by the mechanism of autophagy, and autophagy deficiency has been shown to associate with the increase of extracellular amyloid plaque burden [69]. The peptide segment could also be involved in the formation of endosomes [12,19], where presumably a trans-membrane configuration will be adopted. Since there might be multiple fates for the Aβ segments right after cleavage, it was valuable to setup *in vitro* model systems (*i.e.* "*external addition*" and "*pre-incorporation*" models) that mimic both cases. Our current results have shown that the Aβ aggregation pathways for these two systems were very distinct in terms of both the fibril structures and the membrane disruption. We were encouraged that all samples prepared using a single protocol but with different lipid mixture components showed a uniform trend in ThT and Rh fluorescence measurements, which means that the *in vitro* model is probably robust for studying the extracellular aggregation of Aβ. However, it was also noticed that the absolute values of fluorescence emissions are different, which indicated that the detailed fibril structures are sensitive to membrane components. Therefore in future tests, it is important to use models that mimic the human brain environments around neurons, and the addition of human brain extracts without amyloid plaques might be helpful [34,57].

The solid state NMR results also provide hints to the aggregation pathway at molecular level. Although the TEM morphologies of the "*external addition*" and "*pre-incorporation*" fibrils were different, their NMR linewidths for the residues Phe19 and Leu34 look similar. This means that in both cases, the peptide conformations at the hydrophobic core regions (*i.e.* C-terminal and N-terminal β strands) were probably defined. However, the molecular interaction that stabilizes the tertiary structure is not established. For instance, the formation of "steric zipper", which has been proposed to be crucial for the amyloid fibril structures, requires hydrophobic interactions between the side chains of several pairs of residue [70,71]. In the presence of membrane bilayers, there might be an energy cost for the formation of such hydrophobic interactions because the Aβ peptides may initially interact with the membrane. Such interaction could become stronger if the samples are prepared in a "*pre-incorporation*" way. Therefore, certain types of intermediate structures may also be stabilized in the presence of the membrane. In addition, different sample preparation protocols may affect the amyloidosis pathway because of the difference in local Aβ concentration. Previous CD and ^{19}F solid state NMR studies have demonstrated the formation of distinct Aβ aggregation intermediates due to the change in the initial protein concentration [72].

5. Conclusion

We monitored the Aβ fibrillation process and the associated membrane disruption using two biologically relevant *in vitro* model systems by TEM, fluorescence spectroscopy and solid state NMR. Our results suggested that the Aβ fibrillation pathways were strongly affected by the initial states of peptides in membrane systems, *i.e.* whether the sample was prepared with the external addition or pre-incorporation of the peptide. These two models may serve as mimics for the biological scenarios of extracellular aggregation of Aβ and formation of endosomes, respectively. For both of these two model systems, the Aβ peptides were proved to be non-fusogenic. Membrane disruption was induced by the initial structural change of the membrane-associated peptides, and possibly through the mechanisms of phospholipid uptake. Elongation of mature fibrils may have less effect on the integrity of membrane bilayers. High resolution studies showed that the long-range contact that stabilizes the hydrophobic core regions of Aβ fibrils may form after the local secondary conformation of peptide backbone. Certain intermediate structures may be stabilized by the interaction between the peptides and membrane.

Acknowledgements

This work was supported by the intramural research program at the National Institutes of Health and the startup research funding from Binghamton University, State University of New York. The NMR experiments on the 600 MHz spectrometer were funded by the NSF Major Research Instrumentation Program (NSF 0922815). We greatly thank Dr. Robert Tycko for his support on using materials and instruments, as well as helpful discussion of the results.

Appendix A. Supplementary data

Supplementary data to this article can be found online at http://dx.doi.org/10.1016/j.bbamem.2014.04.011.

References

[1] B.A. Yankner, T. Lu, Amyloid beta-protein toxicity and the pathogenesis of Alzheimer disease, J. Biol. Chem. 284 (2009) 4754–4758.
[2] R.E. Tanzi, L. Bertram, Twenty years of the Alzheimer's disease amyloid hypothesis: a genetic perspective, Cell 120 (2005) 545–555.
[3] C. Haass, D.J. Selkoe, Soluble protein oligomers in neurodegeneration: lessons from the Alzheimer's amyloid beta-peptide, Nat. Rev. Mol. Cell Biol. 8 (2007) 101–112.
[4] D.J. Selkoe, The molecular pathology of Alzheimer's-disease, Neuron 6 (1991) 487–498.
[5] R. Postina, A closer look at alpha-secretase, Curr. Alzheimer Res. 5 (2008) 179–186.
[6] M. Deuss, K. Reiss, D. Hartmann, Part-time alpha-secretases: the functional biology of ADAM 9, 10 and 17, Curr. Alzheimer Res. 5 (2008) 187–201.
[7] P.J. Barrett, Y. Song, W.D. Van Horn, E.J. Hustedt, J.M. Schafer, A. Hadziselimovic, A.J. Beel, C.R. Sanders, The amyloid precursor protein has a flexible transmembrane domain and binds cholesterol, Science 336 (2012) 1168–1171.
[8] G.P. Eckert, W.G. Wood, W.E. Mueller, Lipid membranes and beta-amyloid: a harmful connection, Curr. Protein Pept. Sci. 11 (2010) 319–325.
[9] A.D. Watt, V.L. Villemagne, K.J. Barnham, Metals, membranes, and amyloid-beta oligomers: key pieces in the Alzheimer's disease puzzle? J. Alzheimers Dis. 33 (2013) S283–S293.
[10] K.S. Vetrivel, G. Thinakaran, Membrane rafts in Alzheimer's disease beta-amyloid production, Biochim. Biophys. Acta Mol. Cell Biol. Lipids 1801 (2010) 860–867.
[11] T. Miura, M. Yoda, C. Tsutsumi, K. Murayama, H. Takeuchi, Conformational regulation of amyloid beta-peptide by lipid membranes and metal ions, Yakugaku Zasshi J. Pharm. Soc. Jpn. 130 (2010) 495–501.
[12] R.P. Mason, J.D. Estermyer, J.F. Kelly, P.E. Mason, Alzheimer's disease amyloid beta peptide 25–35 is localized in the membrane hydrocarbon core: X-ray diffraction analysis, Biochem. Biophys. Res. Commun. 222 (1996) 78–82.
[13] J. McLaurin, A. Chakrabartty, Characterization of the interactions of Alzheimer beta-amyloid peptides with phospholipid membranes, Eur. J. Biochem. 245 (1997) 355–363.
[14] M.-S. Lin, X.-B. Chen, S.S.S. Wang, Y. Chang, W.-Y. Chen, Dynamic fluorescence imaging analysis to investigate the cholesterol recruitment in lipid monolayer during the interaction between beta-amyloid (1–40) and lipid monolayers, Colloids Surf. B: Biointerfaces 74 (2009) 59–66.
[15] M.J.O. Widenbrant, J. Rajadas, C. Sutardja, G.G. Fuller, Lipid-induced beta-amyloid peptide assemblage fragmentation, Biophys. J. 91 (2006) 4071–4080.
[16] P.T. Wong, J.A. Schauerte, K.C. Wisser, H. Ding, E.L. Lee, D.G. Steel, A. Gafni, Amyloid-beta membrane binding and permeabilization are distinct processes influenced separately by membrane charge and fluidity, J. Mol. Biol. 386 (2009) 81–96.
[17] H. Yamaguchi, M.L.C. Maat-Schieman, S.G. van Duinen, F.A. Prins, P. Neeskens, R. Natte, R.A.C. Roos, Amyloid beta protein (A beta) starts to deposit as plasma membrane-bound form in diffuse plaques of brains from hereditary cerebral hemorrhage with amyloidosis-Dutch type, Alzheimer disease and nondemented aged subjects, J. Neuropathol. Exp. Neurol. 59 (2000) 723–732.
[18] N. Oshima, M. Morishima-Kawashima, H. Yamaguchi, M. Yoshimura, S. Sugihara, K. Khan, D. Games, D. Schenk, Y. Ihara, Accumulation of amyloid beta-protein in the low-density membrane domain accurately reflects the extent of beta-amyloid deposition in the brain, Am. J. Pathol. 158 (2001) 2209–2218.
[19] R.P. Mason, R.F. Jacob, M.F. Walter, P.E. Mason, N.A. Avdulov, S.V. Chochina, U. Igbavboa, W.G. Wood, Distribution and fluidizing action of soluble and aggregated amyloid beta-peptide in rat synaptic plasma membranes, J. Biol. Chem. 274 (1999) 18801–18807.
[20] W.E. Muller, G.P. Eckert, K. Scheuer, N.J. Cairns, A. Maras, W.F. Gattaz, Effects of beta-amyloid peptides on the fluidity of membranes from frontal and parietal lobes of human brain. High potencies of A beta 1–42 and A beta 1–43, Int. J. Experiment. Clin. Investig. 5 (1998) 10–15.
[21] G.P. Eckert, N.J. Cairns, A. Maras, W.F. Gattaz, W.E. Muller, Cholesterol modulates the membrane-disordering effects of beta-amyloid peptides in the hippocampus: specific changes in Alzheimer's disease, Dement. Geriatr. Cogn. Disord. 11 (2000) 181–186.
[22] I. Peters, U. Igbavboa, T. Schuett, S. Haidari, U. Hartig, X. Rosello, S. Boettner, E. Copanaki, T. Deller, D. Koegel, W.G. Wood, W.E. Mueller, G.P. Eckert, The interaction of beta-amyloid protein with cellular membranes stimulates its own production, Biochim. Biophys. Acta Biomembr. 1788 (2009) 964–972.
[23] C.J. Pike, A.J. Walencewicz, C.G. Glabe, C.W. Cotman, Aggregation-related toxicity of synthetic beta-amyloid protein in hippocampal cultures, Eur. J. Pharmacol. Mol. Pharmacol. Sect. 207 (1991) 367–368.
[24] E. Terzi, G. Holzemann, J. Seelig, Interaction of Alzheimer beta-amyloid peptide(1–40) with lipid membranes, Biochemistry 36 (1997) 14845–14852.
[25] J. Brender, S. Salamekh, A. Ramamoorthy, Membrane-disruption and early events in the aggregation of the diabetes related peptide IAPP from a molecular perspective, Acc. Chem. Res. 116 (2012) 3650–3658.
[26] A. Ramamoorthy, Insights into protein misfolding and amyloidogenesis, Phys. Chem. Chem. Phys. 15 (2013) 8867-8867.
[27] A. Ramamoorthy, Beyond NMR, spectra of antimicrobial peptides: dynamical images at atomic resolution and functional insights, Solid State Nucl. Magn. Reson. 35 (2009) 201–207.
[28] S. Ravault, O. Soubias, O. Saurel, A. Thomas, R. Brasseur, A. Milon, Fusogenic Alzheimer's peptide fragment A beta (29–42) in interaction with lipid bilayers: secondary structure, dynamics, and specific interaction with phosphatidylethanolamine polar heads as revealed by solid-state NMR, Protein Sci. 14 (2005) 1181–1189.
[29] T.L. Lau, E.E. Ambroggio, D.J. Tew, R. Cappai, C.L. Masters, G.D. Fidelio, K.J. Barnham, F. Separovic, Amyloid-beta peptide disruption of lipid membranes and the effect of metal ions, J. Mol. Biol. 356 (2006) 759–770.
[30] S.V. Chochina, N.A. Avdulov, U. Igbavboa, J.P. Cleary, E.O. O'Hare, W.G. Wood, Amyloid beta-peptide (1–40) increases neuronal membrane fluidity: role of cholesterol and brain region, J. Lipid Res. 42 (2001) 1292–1297.
[31] N.A. Avdulov, S.V. Chochina, U. Igbavboa, E.O. Ohare, F. Schroeder, J.P. Cleary, W.G. Wood, Amyloid beta-peptides increase annular and bulk fluidity and induce lipid peroxidation in brain synaptic plasma membranes, J. Neurochem. 68 (1997) 2086–2091.
[32] A.K. Paravastu, R.D. Leapman, W.-M. Yau, R. Tycko, Molecular structural basis for polymorphism in Alzheimer's beta-amyloid fibrils, Proc. Natl. Acad. Sci. 105 (2008) 18349–18354.
[33] A.K. Paravastu, A.T. Petkova, R. Tycko, Polymorphic fibril formation by residues 10–40 of the Alzheimer's beta-amyloid peptide, Biophys. J. 90 (2006) 4618–4629.
[34] A.K. Paravastu, I. Qahwash, R.D. Leapman, S.C. Meredith, R. Tycko, Seeded growth of beta-amyloid fibrils from Alzheimer's brain-derived fibrils produces a distinct fibril structure, Proc. Natl. Acad. Sci. 106 (2009) 7443–7448.
[35] W. Qiang, W.-M. Yau, R. Tycko, Structural evolution of Iowa mutant beta-amyloid fibrils from polymorphic to homogeneous states under repeated seeded growth, J. Am. Chem. Soc. 133 (2011) 4018–4029.
[36] R. Tycko, Solid-State NMR Studies of Amyloid Fibril Structure, in: S.R. Leone, P.S. Cremer, J.T. Groves, M.A. Johnson (Eds.), Annu. Rev. Phy. Chem., vol. 62, 2011, pp. 279–299, (Vol 62).
[37] R. Tycko, Progress towards a molecular-level structural understanding of amyloid fibrils, Curr. Opin. Struct. Biol. 14 (2004) 96–103.
[38] R. Tycko, Insights into the amyloid folding problem from solid-state NMR, Biochemistry 42 (2003) 3151–3159.
[39] R. Tycko, R.B. Wickner, Molecular structures of amyloid and prion fibrils: consensus versus controversy, Acc. Chem. Res. 46 (2013) 1487–1496.
[40] H. Hayashi, T. Mizuno, M. Michikawa, C. Haass, K. Yanagisawa, Amyloid precursor protein in unique cholesterol-rich microdomains different from caveolae-like domains, Biochim. Biophys. Acta Mol. Cell Biol. Lipids 1483 (2000) 81–90.
[41] M. Bokvist, F. Lindstrom, A. Watts, G. Grobner, Two types of Alzheimer's beta-amyloid (1–40) peptide membrane interactions: aggregation preventing transmembrane anchoring versus accelerated surface fibril formation, J. Mol. Biol. 335 (2004) 1039–1049.
[42] M.F.M. Engel, L. Khemtemourian, C.C. Kleijer, H.J.D. Meeldijk, J. Jacobs, A.J. Verkleij, B. de Kruijff, J.A. Killian, J.W.M. Hoeppener, Membrane damage by human islet amyloid polypeptide through fibril growth at the membrane, Proc. Natl. Acad. Sci. 105 (2008) 6033–6038.
[43] M.F. Sciacca, J.R. Brender, D.K. Lee, A. Ramamoorthy, Phosphatidylethanolamine enhances amyloid fiber-dependent membrane fragmentation, Biochemistry 51 (2012) 7676–7684.
[44] C.M. Gabrys, W. Qiang, Y. Sun, L. Xie, S.D. Schmick, D.P. Weliky, Solid-state nuclear magnetic resonance measurements of HIV fusion peptide (CO)-C-13 to lipid P-31 proximities support similar partially inserted membrane locations of the alpha helical and beta sheet peptide structures, J. Phys. Chem. A 117 (2013) 9848–9859.
[45] W. Qiang, Y. Sun, D.P. Weliky, A strong correlation between fusogenicity and membrane insertion depth of the HIV fusion peptide, Proc. Natl. Acad. Sci. 106 (2009) 15314–15319.
[46] R.V. Pappu, X. Wang, A. Vitalis, S.L. Crick, A polymer physics perspective on driving forces and mechanisms for protein aggregation, Arch. Biochem. Biophys. 469 (2008) 132–141.
[47] G. Wei, W. Song, P. Derreumaux, N. Mousseau, Self-assembly of amyloid-forming peptides by molecular dynamics simulations, Front. Biosci. 13 (2008) 5681–5692.
[48] W. Qiang, K. Kelley, R. Tycko, Polymorph-specific kinetics and thermodynamics of beta-amyloid fibril growth, J. Am. Chem. Soc. 135 (2013) 6860–6871.
[49] R. Tycko, K.L. Sciarretta, J.P.R.O. Orgel, S.C. Meredith, Evidence for novel beta-sheet structures in Iowa mutant beta-amyloid fibrils, Biochemistry 48 (2009) 6072–6084.
[50] R. Kodali, A.D. Williams, S. Chemuru, R. Wetzel, A beta (1–40) forms five distinct amyloid structures whose beta-sheet contents and fibril stabilities are correlated, J. Mol. Biol. 401 (2010) 503–517.
[51] M.P. Mingeot-Leclercq, L. Lins, M. Bensliman, F. Van Bambeke, P. Van der Smissen, J. Peuvot, A. Schanck, R. Brasseur, Membrane destabilization induced by beta-amyloid peptide 29–42: importance of the amino-terminus, Chem. Phys. Lipids 120 (2002) 57–74.
[52] A. Laganowsky, C. Liu, M.R. Sawaya, J.P. Whitelegge, J. Park, M. Zhao, A. Pensalfini, A.B. Soriaga, M. Landau, P.K. Teng, D. Cascio, C. Glabe, D. Eisenberg, Atomic view of a toxic amyloid small oligomer, Science 335 (2012) 1228–1231.
[53] S. Lee, D. Eisenberg, Seeded conversion of recombinant prion protein to a disulfide-bonded oligomer by a reduction–oxidation process, Nat. Struct. Biol. 10 (2003) 725–730.
[54] E. Sparr, M.F.M. Engel, D.V. Sakharov, M. Sprong, J. Jacobs, B. de Kruijff, J.W.M. Hoppener, J.A. Killian, Islet amyloid polypeptide-induced membrane leakage involves uptake of lipids by forming amyloid fibers, FEBS Lett. 577 (2004) 117–120.
[55] M.F.M. Sciacca, S.A. Kotler, J.R. Brender, J. Chen, D.K. Lee, A. Ramamoorthy, Two step mechanism of membrane disruption by Aβ through membrane fragmentation and pore formation, Biophys. J. 103 (2012) 702–710.

[56] S.A. Kotler, P. Walsh, J.R. Breander, A. Ramamoorthy, Differences between amyloid-beta aggregation in solution and on the membrane: insights in to elucidation of the mechanistic details of Alzheimer's disease, Chem. Soc. Rev. (2014), http://dx.doi.org/10.1039/C3CS60431D.
[57] J.-X. Lu, W. Qiang, W.-M. Yau, C.D. Schwieters, S.C. Meredith, R. Tycko, Molecular structure of beta-amyloid fibrils in Alzheimer's disease brain tissue, Cell 154 (2013) 1257–1268.
[58] A.T. Petkova, W.M. Yau, R. Tycko, Experimental constraints on quaternary structure in Alzheimer's beta-amyloid fibrils, Biochemistry 45 (2006) 498–512.
[59] W. Qiang, W.-M. Yau, Y. Luo, M.P. Mattson, R. Tycko, Antiparallel beta-sheet architecture in Iowa-mutant beta-amyloid fibrils, Proc. Natl. Acad. Sci. 109 (2012) 4443–4448.
[60] M. Biancalana, S. Koide, Molecular mechanism of thioflavin-T binding to amyloid fibrils, Biochim. Biophys. Acta Protein Proteomics 1804 (2010) 1405–1412.
[61] C. Wu, M. Biancalana, S. Koide, J.-E. Shea, Binding modes of thioflavin-T to the single-layer beta-sheet of the peptide self-assembly mimics, J. Mol. Biol. 394 (2009) 627–633.
[62] R. Kayed, E. Head, J.L. Thompson, T.M. McIntire, S.C. Milton, C.W. Cotman, C.G. Glabe, Common structure of soluble amyloid oligomers implies common mechanism of pathogenesis, Science 300 (2003) 486–489.
[63] I. Benilova, E. Karran, B. De Strooper, The toxic A beta oligomer and Alzheimer's disease: an emperor in need of clothes, Nat. Neurosci. 15 (2012) 349–357.
[64] S.E. Lesne, M.A. Sherman, M. Grant, M. Kuskowski, J.A. Schneider, D.A. Bennett, K.H. Ashe, Brain amyloid-beta oligomers in ageing and Alzheimer's disease, Brain 136 (2013) 1383–1398.
[65] A.T. Petkova, R.D. Leapman, Z.H. Guo, W.M. Yau, M.P. Mattson, R. Tycko, Self-propagating, molecular-level polymorphism in Alzheimer's beta-amyloid fibrils, Science 307 (2005) 262–265.
[66] K.-N. Hu, W.-M. Yau, R. Tycko, Detection of a transient intermediate in a rapid protein folding process by solid-state nuclear magnetic resonance, J. Am. Chem. Soc. 132 (2010) 24–25.
[67] H.A. Scheidt, I. Morgado, D. Huster, Solid-state NMR reveals a close structural relationship between amyloid-beta protofibrils and oligomers, J. Biol. Chem. 287 (2012) 22822–22826.
[68] A. Quist, L. Doudevski, H. Lin, R. Azimova, D. Ng, B. Frangione, B. Kagan, J. Ghiso, R. Lal, Amyloid ion channels: a common structural link for protein-misfolding disease, Proc. Natl. Acad. Sci. 102 (2005) 10427–10432.
[69] P. Nilsson, K. Loganathan, M. Sekiguchi, Y. Matsuba, K. Hui, S. Tsubuki, M. Tanaka, N. Iwata, T. Saito, T.C. Saido, A beta secretion and plaque formation depend on autophagy, Cell Rep. 5 (2013) 61–69.
[70] C. Liu, M.R. Sawaya, P.-N. Cheng, J. Zheng, J.S. Nowick, D. Eisenberg, Characteristics of amyloid-related oligomers revealed by crystal structures of macrocyclic beta-sheet mimics, J. Am. Chem. Soc. 133 (2011) 6736–6744.
[71] S.A. Sievers, J. Karanicolas, H.W. Chang, A. Zhao, L. Jiang, O. Zirafi, J.T. Stevens, J. Muench, D. Baker, D. Eisenberg, Structure-based design of non-natural amino-acid inhibitors of amyloid fibril formation, Nature 475 (2011) 96-U117.
[72] Y. Suzuki, J.R. Brender, M.T. Soper, J. Krishnamoorthy, Y. Zhou, B.T. Ruotolo, N.A. Kotov, A. Ramamoorthy, E.N. Marsh, Resolution of oligomeric species during the aggregation of Abeta1–40 using 19F NMR, Biochemistry 52 (2013) 1903–1912.